Journal of Zhejiang University-SCIENCE A (Applied Physics & Engineering)
ISSN 1673-565X (Print); ISSN 1862-1775 (Online)
www.jzus.zju.edu.cn; www.springerlink.com
E-mail: jzus@zju.edu.cn

Geometric state transfer method for construction control of a large-segment steel box girder with hoisting installation*

Jin-feng WANG†, Hua-wei XIANG, Jiang-tao ZHANG, Tian-mei WU, Rong-qiao XU

College of Civil Engineering and Architecture, Zhejiang University, Hangzhou 310058, China

†E-mail: wangjinfeng@zju.edu.cn

Received June 16, 2019; Revision accepted Nov. 8, 2019; Crosschecked Mar. 17, 2020

Abstract: This paper aims to address the problem of geometric state control of large-segment steel box girders in offshore hoisting during the construction of large-span bridges. First, the geometric state control indexes of a large-segment steel box girder are determined, such as the manufacturing parameters of the top and bottom slabs, the width of the annular joint, and the support position. Second, the geometric state equations and state transfer matrixes of large-segment steel box girders under different conditions are deduced by taking the mileage and elevation of control points as basic state variables. In application of the geometric state transfer method in the construction control of the Hong Kong-Zhuhai-Macao Bridge, the width of the annular joint and the position parameters for the support of the large-segment steel box girder are predicted precisely. Moreover, the manufacturing parameters of the top and bottom slabs of the steel box girders are calculated reliably. The measured values show that the width of the annular joint is basically the same with the difference of less than 2 mm, the eccentricity of bridge support is less than 20 mm, and the elevation error of the bridge deck is within −10 mm to +15 mm, which meets the construction accuracy. Using the geometric state transfer method, the rapid and accurate installation of the Hong Kong-Zhuhai-Macao Bridge has been realized, demonstrating that the precise control of the geometric state of a steel box girder with ectopic installation and multi-state transition can be realized by using the geometric state transfer method.

Key words: Large-segment steel box girder; Offshore hoisting; Construction control; Geometric state; Transfer matrix
https://doi.org/10.1631/jzus.A1900213 **CLC number:** U445

1 Introduction

To achieve high construction efficiency, the hoisting construction of large-segment steel box girders, which can install beams over 100 m in length at a time, has become very popular in recent years for bridge engineering under severe natural conditions such as sea-crossings, river-crossings, and complex urban environmental conditions (Meng et al., 2014). With this construction method, large-segment steel box girders have to go through the construction stages of factory manufacture, site installation, bridge connection, and so on. Consequently, the geometric states of a bridge change considerably at its various construction stages. Moreover, high precision in the elevation of the bridge deck, the smoothness of large-segment annular joints, and the positioning of bridge supports are required and pose a great challenge to construction control.

Open-loop control, closed-loop control, and self-adaptive control have been used widely for control of bridge construction (Li Q et al., 2009; Yan et al., 2012; Li CX et al., 2015). Muller (1975) emphasized that the calculation of bridge deflection is of great significance for the realization of bridge configuration. Zhong et al. (1992) used the open-loop control

* Project supported by the Zhejiang Provincial Natural Science Foundation of China (No. LZ16E080001) and the National Natural Science Foundation of China (Nos. 51578496 and 51878603)
ORCID: Jin-feng WANG, https://orcid.org/0000-0002-9099-818X
© Zhejiang University and Springer-Verlag GmbH Germany, part of Springer Nature 2020

method to conduct construction control of a single-tower cable-stayed pipe bridge and achieved satisfactory results. However, the open-loop control method just sets theoretical parameters without considering subsequent errors, which leaves the issue of error accumulation. For this reason, the closed-loop control method was developed. This method considers construction errors and adjusts them by feedback analysis. In China, Lin (1983) applied the closed-loop control method for the first time—in the construction of the Shanghai Maogang Bridge. The configuration error of the bridge was controlled within 2 cm. Breen (1985) used the closed-loop control method to implement geometric state control of a prestressed concrete continuous beam bridge with segmentally assembled construction. Since then, the same method has been adopted for the construction of the Annasis Bridge in Canada (Taylor, 1986) and the Yokohama Bay Bridge in Japan (Wada et al., 1991).

The closed-loop control method cannot be used to predict errors in advance; thus, error adjustment must be carried out according to a certain optimal state after the error appears. To implement active control of errors, parameter identification was introduced into the closed-loop control method to form a self-adaptive control method. For the cantilever construction of a bridge, the design parameters are identified and corrected using measurement data during construction, so that the calculated value of the model can reflect the actual structural response more accurately in the subsequent construction step, thus achieving accurate control of construction. Seki and Tanaka (1991) developed a self-adaptive system for the construction control of a cable-stayed bridge and used this system for construction control of the Tomei Ashigara Bridge. Chen et al. (1993) proposed the least square method for parameter identification of a cable-stayed bridge and applied it to the construction control of the Ningbo Yongjiang Bridge (a concrete cable-stayed bridge). Li et al. (2009) established a full-process self-adaptive geometric control system for the construction control of Sutong Bridge. Previous studies have shown that the self-adaptive control method can achieve reasonable results in the construction of cable-stayed bridges with segment cantilevers.

Compared with bridges constructed with a small-segment cantilever, the geometric state of the steel box girders with whole-span ectopic installation varies continuously from factory manufacture to offshore installation and the completion of the bridge. Meanwhile, errors in the whole-span ectopic installation cannot be adjusted step-by-step as is done in small-segment cantilever construction. For the construction control of steel box girders installed over the whole span, it is essential to control the geometric state accurately after the stress analysis in the construction process, which requires determining the transitive among the geometric states. The transfer matrix method was originally used to solve the static and dynamic problems of elastic structures (Thomson, 1950). Rosignoli (1997) successfully applied this method to the analysis of the incremental launching construction of a straight bridge. Arici and Granata (2007) further applied the method to the analysis of the incremental launching construction of a curved bridge. Based on the basic idea of the transfer matrix method, Lin et al. (2014) and Wang et al. (2015) put forward the idea of transferring the geometric state to conduct construction control of a steel channel girder constructed by the incremental launching method. This was successfully applied to the construction control of the Jiubao Bridge in Hangzhou.

This paper proposes a geometric state transfer method using the mileage and elevation of steel box girder control points as the basic state variables. First, the geometric state control indexes of a large-segment steel box girder are determined, including the length of the top and bottom slabs, the width of the large-segment annular joints, and the positioning of the bridge supports. Second, the geometric state equations and geometric state transfer matrixes of large-segment steel box girders under different states are deduced, and the method for the calculation of control indexes is given. Finally, this method is applied to the geometric state control of the large-segment steel box girder of the non-navigable section of the Hong Kong-Zhuhai-Macao Bridge. Using this method, the manufacturing parameters of the steel box girder were calculated accurately, the difference in the weld width between the top and bottom slabs of the large-segment steel box girder was controlled precisely, and the positioning parameters of the supports were predicted accurately.

2 Project background

The Hong Kong-Zhuhai-Macao Bridge project is a large-scale sea-crossing project integrating bridges, artificial islands, and immersed tunnels. Its total length is about 55 km, and the length of the main bridges is about 22.9 km. In the non-navigable deep sea, the bridge adopts a continuous steel box girder style with six spans (Fig. 1a). The section of the steel box girder is a single box with a double-chamber. The height of the girder is 4.50 m and the width of the top slab is 33.10 m (Fig. 1b). In the factory manufacturing stage, small-segments of about 10 m in length were assembled from plate elements and then large-segments of about 110 m in length were assembled from the small-segments (Fig. 2). For the offshore construction stage, a large-segment hoisting construction method was used. The longest segment hoisted was 132.6 m in length and about 3200 t in weight. The latest large-segment steel box girder is temporarily supported by a corbel to the former one, which has been hoisted into place (Fig. 2). After the steel box girders were installed in the appropriate position, the annular joint is connected by bolting and welding; the standard width of the annular joint is 6–8 mm.

The assembly construction method was adopted in the Hong Kong-Zhuhai-Macao Bridge project. The method requires very high-precision construction control: the elevation error of the bridge deck should be well controlled (−10 to +20 mm), the width difference of the annular joint between the top and bottom of the large-segment should not exceed 2 mm, and the eccentricity of the support on the steel box girder should not exceed 20 mm on the pier padstone. In order to achieve such high-precision control, it is necessary to strictly control the manufacturing parameters of the top and bottom slabs of the steel box girders during manufacture, the width of the large-segment annular joint, and the positioning parameters of the supports for the large-segment steel box girders during offshore installation.

3 Geometric state control method

3.1 Analysis of the geometric state

The change in the internal force states of a bridge during construction can be reflected in the change in its geometric shape. Despite the fact that the measuring accuracy of the geometric state of the structure is much more important than that of the internal forces, the control of the geometric state of the steel box girder not only ensures realization of the design alignment, but also ensures realization of the design internal force state of the bridge. During construction, the geometric states of a large-segment steel box girder change constantly from factory manufacture to final installation. The typical geometric states in the construction are the designed bridge state (the mileage and elevation given in design drawings of the bridge), stress-free state, factory assembly state, and installation state, which are expressed by $\boldsymbol{\Phi}^{\mathrm{D}}$, $\boldsymbol{\Phi}^{\mathrm{N}}$, $\boldsymbol{\Phi}^{\mathrm{C}}$,

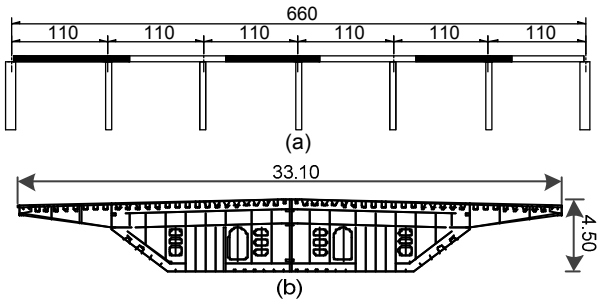

Fig. 1 Schematic diagram of non-navigable bridge in the deep sea of the Hong Kong-Zhuhai-Macao Bridge (unit: m)

(a) Schematic diagram of standard span arrangement and large-segment division; (b) Schematic diagram of cross-section of steel box girder

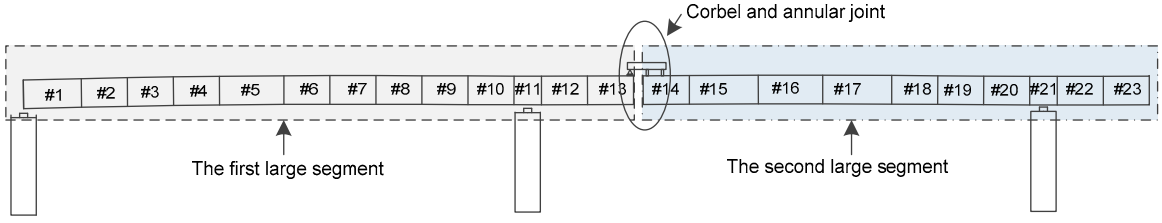

Fig. 2 Division of small-segments in the large-segments and the corbel arrangement (only the first two large-segments are listed)

and $\boldsymbol{\Phi}^{\mathrm{H}}$, respectively. The transition relationship among these states is shown in Fig. 3.

3.2 State control variables

The mileage and elevation of each point during bridge engineering, provide the basic geometric information for a structure. These are easily measured and related to the calculations of deformation of the structure. Therefore, the mileage and elevation of each control point on the steel box girder were selected as the geometric state variables. The coordinate of the control point is $[S_i\ H_i]^{\mathrm{T}}$, where S_i and H_i are the mileage and elevation of control point P_i, respectively.

Six control points were selected for a single small-segment steel box girder. These were located on the neutral axis, and on the top and the bottom of the steel box girder (Fig. 4). Using these control points, the manufacturing parameters of the top and bottom slabs, the width of the annular joint, and the position of the support can be calculated.

The meanings of the symbols in Fig. 4 are as follows: P_i is the control point on the neutral axis of the ith beam segment. P_i^1, P_i^3, and P_i^2, P_i^4 are the control points of the top and bottom slabs of the ith beam segment, respectively. h_i^{s} and h_{i+1}^{s} are the distances from the upper edge of the left and right end of the ith beam segment to the neutral axis position of the section, respectively. h_i^{x} and h_{i+1}^{x} are the distances from the lower edge of the left and right end of the ith beam segment to the neutral axis position of the section, respectively. L_i is the length of the neutral axis of the ith beam segment. The term α_i is the angle between the ith beam segment and the horizontal line. The above parameters are given in the design drawings.

3.3 State transfer

The geometric states of a large-segment steel box girder change from factory manufacture to bridge site installation until completion of the bridge. There are two key states among these geometric states: the stress-free state and the designed bridge state. The stress-free state is the initial state in the construction and the designed bridge state is the target state of construction. Other intermediate states can be obtained from the stress-free state. First, information on the designed bridge state (mileage, elevation, and structural geometries) is given in the bridge design drawings. Then, the stress-free state can be determined according to the structural analysis of the designed bridge state, and the relationship between them can be expressed as follows.

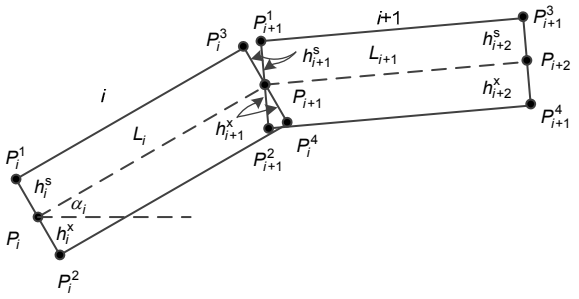

Fig. 4 Control points for small-segment steel box girder in elevation view

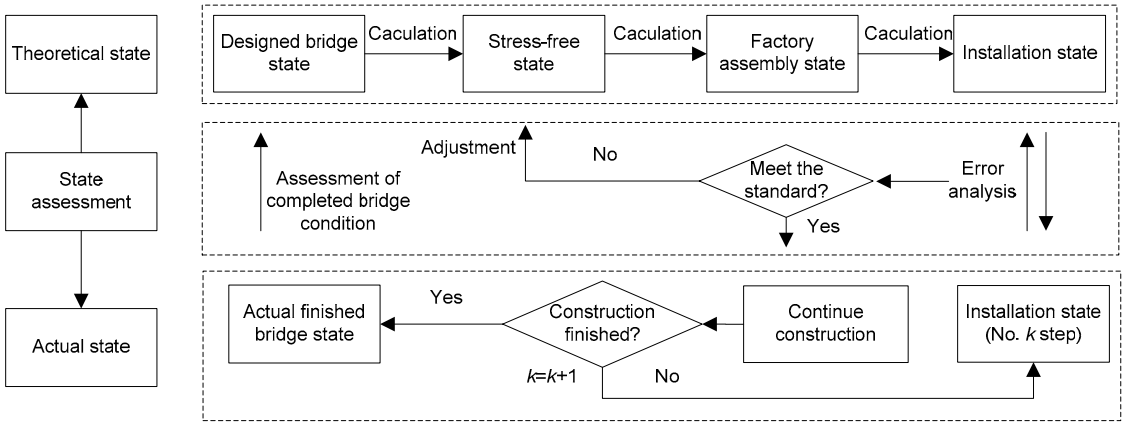

Fig. 3 Relationship among different states of a large-segment steel box girder

$$\boldsymbol{\Phi}^{\mathrm{N}}=\boldsymbol{\Phi}^{\mathrm{D}}+\Delta^{\mathrm{D}}=\left[\boldsymbol{\Phi}_i^{\mathrm{N}}\right]_{i=1,2,\ldots,n}=\begin{bmatrix}\boldsymbol{\Phi}_1^{\mathrm{D}}+\Delta_1^{\mathrm{D}}\\ \boldsymbol{\Phi}_2^{\mathrm{D}}+\Delta_2^{\mathrm{D}}\\ \vdots\\ \boldsymbol{\Phi}_n^{\mathrm{D}}+\Delta_n^{\mathrm{D}}\end{bmatrix}, \quad (1)$$

where n is the number of small-segment steel box girders and Δ^{D} is the design pre-camber, which can be obtained by structural calculation.

In Fig. 4, P_i represents the base point of the ith beam segment. The state relations of the remaining control points relate to the base point in the segment and can be determined by geometric relations. Then, the state vector of the beam segment is formed by the state vector of six points (P_i, P_i^1, P_i^2, P_{i+1}, P_i^3, and P_i^4) together.

$$\boldsymbol{\Phi}_i^{\mathrm{N}}=\begin{bmatrix}\boldsymbol{P}_i^{\mathrm{N}}\\ \boldsymbol{\Psi}_i^{\mathrm{N}}\end{bmatrix}, \quad (2)$$

where $\boldsymbol{P}_i^{\mathrm{N}}=\begin{bmatrix}S_i^{\mathrm{N}} & H_i^{\mathrm{N}}\end{bmatrix}^{\mathrm{T}}$, and $\boldsymbol{\Psi}_i^{\mathrm{N}}$ is a vector of control points other than the base point, and it can be represented as

$$\begin{aligned}\boldsymbol{\Psi}_i^{\mathrm{N}}=&\begin{bmatrix}\boldsymbol{I}_2 & \boldsymbol{I}_2 & \boldsymbol{I}_2 & \boldsymbol{I}_2 & \boldsymbol{I}_2\end{bmatrix}^{\mathrm{T}}\boldsymbol{P}_i^{\mathrm{N}}\\ &+\begin{bmatrix}-\sin\alpha_i & 0 & 0 & 0 & 0\\ \cos\alpha_i & 0 & 0 & 0 & 0\\ 0 & \sin\alpha_i & 0 & 0 & 0\\ 0 & -\cos\alpha_i & 0 & 0 & 0\\ 0 & 0 & \cos\alpha_i & 0 & 0\\ 0 & 0 & \sin\alpha_i & 0 & 0\\ 0 & 0 & \cos\alpha_i & -\sin\alpha_i & 0\\ 0 & 0 & \sin\alpha_i & \cos\alpha_i & 0\\ 0 & 0 & \cos\alpha_i & 0 & \sin\alpha_i\\ 0 & 0 & \sin\alpha_i & 0 & -\cos\alpha_i\end{bmatrix}\begin{bmatrix}h_i^{\mathrm{s}}\\ h_i^{\mathrm{x}}\\ L_i\\ h_{i+1}^{\mathrm{s}}\\ h_{i+1}^{\mathrm{x}}\end{bmatrix},\end{aligned} \quad (3)$$

where $\boldsymbol{I}_2=\begin{bmatrix}1 & 0\\ 0 & 1\end{bmatrix}$ and $\alpha_i=\arctan\left(\dfrac{H_i^{\mathrm{N}}-H_{i+1}^{\mathrm{N}}}{S_i^{\mathrm{N}}-S_{i+1}^{\mathrm{N}}}\right)$.

Using the length and angle of the ith beam segment, the mileage and elevation of the adjacent point in the ith beam segment can be deduced as follows:

$$\boldsymbol{P}_{i+1}^{\mathrm{N}}=\boldsymbol{P}_i^{\mathrm{N}}+L_i\begin{bmatrix}\cos\alpha_i & \sin\alpha_i\end{bmatrix}^{\mathrm{T}},\ i=1,2,\cdots,n. \quad (4)$$

By substituting Eq. (4) into Eq. (2), the state vectors of the (i+1)th beam segment $\boldsymbol{\Phi}_{i+1}^{\mathrm{N}}$ can be obtained. By analogy, the state vectors of the complete large-segment steel box girder can be obtained.

$\boldsymbol{\Phi}^{\mathrm{P}}$ are the predicted state vectors of any intermediate state in the construction of large-segment steel box girders that can be expressed by the stress-free state vectors and the predicted deformation:

$$\boldsymbol{\Phi}^{\mathrm{P}}=\boldsymbol{\Phi}^{\mathrm{N}}+\Delta^{\mathrm{E}}, \quad (5)$$

where Δ^{E} is the theoretical value of the deformation of a beam segment in the intermediate state.

The ambient temperature and the weld shrinkage may not be consistent with the values specified in the design when the steel box girders are assembled. After considering these influencing factors, the factory assembly state can be represented as

$$\boldsymbol{\Phi}_i^{\mathrm{C}}=\boldsymbol{\Phi}_i^{\mathrm{N}}+\boldsymbol{\Delta}_i^{\mathrm{C}}, \quad (6)$$

$$\boldsymbol{\Delta}_i^{\mathrm{C}}=\boldsymbol{\Delta}_i^{\mathrm{CT}}+\boldsymbol{\Delta}_i^{\mathrm{CW}}, \quad (7)$$

$$\boldsymbol{\Delta}_i^{\mathrm{CT}}=\left[\mu(t-t_0)L_i\right]\begin{bmatrix}\boldsymbol{I}_2 & \boldsymbol{I}_2 & \boldsymbol{I}_2 & \boldsymbol{I}_2 & \boldsymbol{I}_2 & \boldsymbol{I}_2\end{bmatrix}^{\mathrm{T}}\begin{bmatrix}\cos\alpha_i\\ \sin\alpha_i\end{bmatrix}, \quad (8)$$

$$\boldsymbol{\Delta}_i^{\mathrm{CW}}=mW_i\begin{bmatrix}\boldsymbol{I}_2 & \boldsymbol{I}_2 & \boldsymbol{I}_2 & \boldsymbol{I}_2 & \boldsymbol{I}_2 & \boldsymbol{I}_2\end{bmatrix}^{\mathrm{T}}\begin{bmatrix}\cos\alpha_i\\ \sin\alpha_i\end{bmatrix}, \quad (9)$$

where $\boldsymbol{\Delta}_i^{\mathrm{CT}}$ is the variation of mileage and elevation due to temperature; $\boldsymbol{\Delta}_i^{\mathrm{CW}}$ is the variation of mileage and elevation due to shrinkage of welds; μ is the thermal expansion coefficient of the material; t is the ambient temperature of the actual assembly state; t_0 is the design reference temperature; m is the total number of circumferential welds in a small segment; W_i is the shrinkage of a single weld at the ith segment.

3.4 Calculation of control parameters

For the large-segment steel box girder, the main control parameters are the length of top and bottom slabs of the girder, the width of the annular joint, and

the support position. With the geometric state equations in each state, the control parameters of large-segment steel box girders can be calculated according to the state vector in the state equation. The calculation method is as follows.

1. Calculation of the manufacturing parameters of a steel box girder

Fig. 5 shows the calculation method for the manufacturing parameters of the top and bottom slabs between sections i and i+1. Only the state vectors of P_i^3, P_i^4 on section i and P_{i+1}^1, P_{i+1}^2 on section i+1 in the stress-free state equation $\boldsymbol{\Phi}^{\mathrm{N}}$ are needed. By approximating the distance $\delta L_i^{\mathrm{t}}=\overrightarrow{P_i^3P_{i+1}^1}^{\mathrm{N}}$ (where $\overrightarrow{P_i^3P_{i+1}^1}^{\mathrm{N}}=\sqrt{(S_i^3|_{\mathrm{N}}-S_{i+1}^1|_{\mathrm{N}})^2+(H_i^3|_{\mathrm{N}}-H_{i+1}^1|_{\mathrm{N}})^2}$) and $\delta L_i^{\mathrm{b}}=\overrightarrow{P_i^4P_{i+1}^2}^{\mathrm{N}}$, the manufacturing parameters of the top and bottom slabs at the connecting end can be determined.

2. Prediction of annular joint width

There is an angle between the annular joints of adjacent large-segment steel box girders in the stress-free state. The width of the top and bottom seams is different (Fig. 6). To predict the width of the annular joint after large-segment hoisting, the stress-free state equation $\boldsymbol{\Phi}^{\mathrm{N}}$ and the predicted deformation Δ^{E} after hoisting are needed. The predicted state equations $\boldsymbol{\Phi}^{\mathrm{P}}$ are obtained from Eq. (5). Using the state vectors of the girder sections #13 and #14 where the annular joints are located, and calculating $\delta D^{\mathrm{t}}=\overrightarrow{P_{13}^3P_{14}^1}^{\mathrm{P}}$ and $\delta D^{\mathrm{b}}=\overrightarrow{P_{13}^4P_{14}^2}^{\mathrm{P}}$, the width of the top and bottom seams at the annular joints can be determined.

3. Support positioning

Supports are installed on the large-segment steel box girder before hoisting. The length of the bottom slab of the steel box girder changes relative to its stress-free state after hoisting, which causes a change of the support position. The change in the length of the bottom slab of the steel box girder should be considered in support positioning. This process is illustrated in Fig. 6. As shown in Fig. 2, the supports are located in the #1 and #11 small-segments of the steel box girder. The distance $\overrightarrow{P_1^2P_{11}^2}^{\mathrm{N}}$ in the stress-free state equation $\boldsymbol{\Phi}^{\mathrm{N}}$ and the distance $\overrightarrow{P_1^2P_{11}^2}^{\mathrm{P}}$ in the state equation $\boldsymbol{\Phi}^{\mathrm{P}}$ are obtained, respectively, at the stage of support installation. The difference between the two distances is the support pre-offset, which can be used to correct the support position in advance.

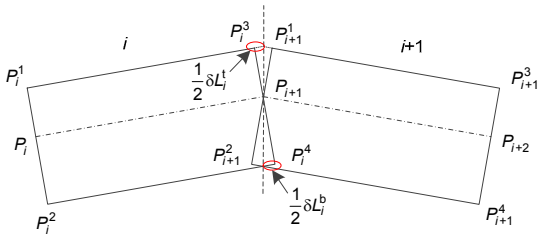

Fig. 5 Top and bottom slabs matching at small-segment joints in elevation view

4 Numerical solutions for the model

The geometric state transfer method was applied to the construction control of large-segment steel box girders in the Hong Kong-Zhuhai-Macao Bridge project. The manufacturing parameters of the top and bottom slabs of the steel box girders were calculated. The width of the annular joints of the large-segment steel box girders and positioning parameters of the supports were predicted.

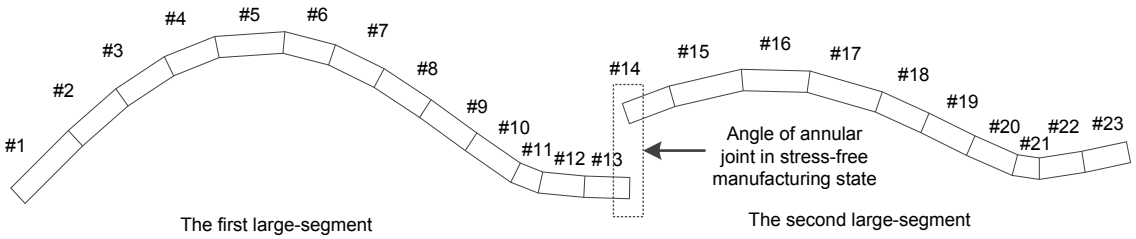

Fig. 6 Angle of the annular joint of the steel box girder in the large-segment steel box girder under stress-free state

4.1 Calculation of the manufacturing parameters of top and bottom slabs of a steel box girder

Taking the first span as an example, Table 1 shows the manufacturing parameters of the top and bottom slabs of a large-segment steel box girder calculated based on state vectors. The large-segment steel box girder of the first span consists of 13 small-segments. Each small-segment is straight and connected by a certain angle to form a large-segment of the curve, which requires adjusting the length of the top and bottom slabs of the large-segment steel box girder to ensure the consistency of the weld width. By using the proposed method, the manufacturing parameters of the top and bottom of each small segment can be easily calculated based on the state vector. For example, the distance $\delta L_2^{\mathrm{t}}=\overrightarrow{P_2^3P_3^1}^{\mathrm{N}}=3$ mm in Table 1 indicates that the joint of #2 and #3 steel box girder top slabs needs to be lengthened by 3 mm, and $\delta L_2^{\mathrm{b}}=\overrightarrow{P_2^4P_3^2}^{\mathrm{N}}=-5$ mm indicates that the joint of the #2 and #3 steel box girder bottom slabs needs to be reduced in length by 5 mm.

4.2 Prediction of annular joint width of a large-segment steel box girder

To predict the annular joint width at the connection of the second large-segment steel box girder after hoisting and the first large-segment steel box girder, it is only necessary to take the state vectors of the #13 and #14 small-segments where the annular joint is located, to do the calculation. The calculation results are shown in Table 2. After the second large-segment steel box girder is hoisted into place, the width of the annular joint in the top position is 8 mm ($\delta D^{\mathrm{t}}=\overrightarrow{P_{13}^3P_{14}^1}^{\mathrm{P}}=8$ mm), and the width of the annular joint in the bottom position is 7 mm ($\delta D^{\mathrm{b}}=\overrightarrow{P_{13}^4P_{14}^2}^{\mathrm{P}}=7$ mm). The difference between them is only 1 mm, which meets the requirement that bolt-welded joints should not exceed 2 mm.

The in situ measured width of the annular joint after the second large-segment steel box girder was hoisted as shown in Fig. 7a. It indicates successful realization of the bolt-welded connection at the annular joint (Fig. 7b).

Table 1 Calculation of the manufacturing parameters of steel box girder in the first span large-segment using the state vectors

Girder section	$(P_i^1)^{\mathrm{N}}$		$(P_i^2)^{\mathrm{N}}$		$(P_i^3)^{\mathrm{N}}$		$(P_i^4)^{\mathrm{N}}$		Matching length (mm)	
	S_i (m)	H_i (m)	S_i (m)	H_i (m)	S_i (m)	H_i (m)	S_i (m)	H_i (m)	δL_i^{t}	δL_i^{b}
#1	−0.043	1.699	0.072	−2.799	12.557	2.022	12.672	−2.477		
#2	12.558	2.022	12.669	−2.477	22.558	2.268	22.669	−2.231	2	−3
#3	22.561	2.268	22.664	−2.231	32.561	2.495	32.664	−2.004	3	−5
#4	32.565	2.495	32.657	−2.004	42.565	2.700	42.657	−1.799	4	−6
#5	42.570	2.700	42.649	−1.799	56.570	2.945	56.649	−1.555	5	−8
#6	56.575	2.945	56.641	−1.555	66.575	3.091	66.641	−1.409	5	−8
#7	66.579	3.091	66.635	−1.409	76.579	3.216	76.635	−1.283	3	−6
#8	76.581	3.217	76.631	−1.283	86.581	3.328	86.631	−1.172	2	−4
#9	86.582	3.328	86.630	−1.172	96.582	3.435	96.630	−1.065	1	−1
#10	96.581	3.435	96.632	−1.065	106.581	3.548	106.632	−0.952	−1	2
#11	106.575	3.548	106.641	−0.952	112.575	3.634	112.641	−0.865	−5	9
#12	112.570	3.634	112.650	−0.865	122.570	3.812	122.650	−0.687	−6	9
#13	122.568	3.812	122.652	−0.687	132.568	3.998	132.652	−0.501	−1	2

Table 2 Prediction of annular joint width of large-segment steel box girder

Girder section	$(P_i^1)^{\mathrm{P}}$		$(P_i^2)^{\mathrm{P}}$		$(P_i^3)^{\mathrm{P}}$		$(P_i^4)^{\mathrm{P}}$		Width (mm)	
	S_i (m)	H_i (m)	S_i (m)	H_i (m)	S_i (m)	H_i (m)	S_i (m)	H_i (m)	δD^{t}	δD^{b}
#13					132.568	4.001	132.652	−0.499	8	7
#14	132.560	4.001	132.645	−0.499						

4.3 Calculation of the support positions

The support displacement is calculated by taking the distance $\overrightarrow{P_1^2P_{11}^2}^{\mathrm{N}}$ in the stress-free state equation $\boldsymbol{\Phi}^{\mathrm{N}}$ and the distance $\overrightarrow{P_1^2P_{11}^2}^{\mathrm{P}}$ in the state equation $\boldsymbol{\Phi}^{\mathrm{P}}$ at the time of support installation. The calculation results are shown in Table 3.

Under the stress-free state $\overrightarrow{P_1^2P_{11}^2}^{\mathrm{N}}=106.585$ m and the relative distance is $\overrightarrow{P_1^2P_{11}^2}^{\mathrm{P}}=106.609$ m after the 2nd large-segment steel box girder is hoisted into place. This means that the elongation of the bottom slab is 24 mm, which needs to be considered in advance in the support pre-offset setting. Otherwise, the eccentricity of the support bottom plate on the pier padstone would exceed the design requirement of 20 mm. After adjusting the pre-offset, the precise installation of the support was realized (Fig. 8).

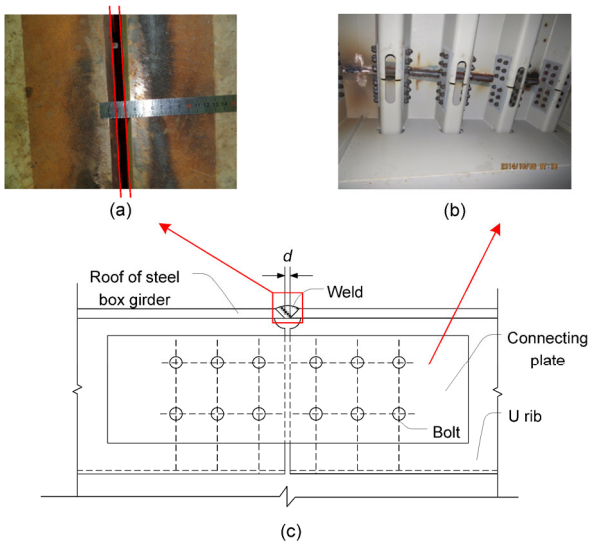

Fig. 7 The second large-segment annular joints connected by bolting and welding

(a) Welding joint of steel box girder roof on site before welding; (b) Photo after annular joint connection; (c) Schematic diagram of bolt-welded connection of large-segment annular joint

4.4 Evaluation of the bridge configuration

Elevation measurements were carried out with a high precision total station under constant temperature conditions, such as before sunrise in the morning (Fig. 9). The actual elevation error of the non-navigable steel box girder bridges of the Hong Kong-Zhuhai-Macao Bridge project was within −10 mm to +15 mm (Fig. 10), which meets its design requirements. Moreover, this indicates that the proposed geometric state transfer method can be used to accurately realize the configuration control of large-segment steel box girders during hoisting construction.

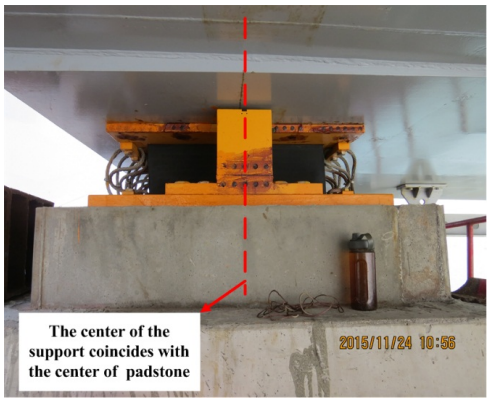

Fig. 8 Photo of the steel box girder support in the large-segment after precise installation



Fig. 9 On-site photo of elevation measurement of steel box girder

Table 3 Prediction of support displacement of large-segment steel box girder

Girder section	$(P_i^2)^{\mathrm{N}}$		$\overrightarrow{P_1^2P_{11}^2}^{\mathrm{N}}$ (m)	$(P_i^2)^{\mathrm{P}}$		$\overrightarrow{P_1^2P_{11}^2}^{\mathrm{P}}$ (m)	Displacement, ΔS (mm)
	S_i (m)	H_i (m)		S_i (m)	H_i (m)		
#1	0.072	−2.799	106.585	0.054	−2.799	106.609	24
#11	106.641	−0.952		106.647	−0.969		

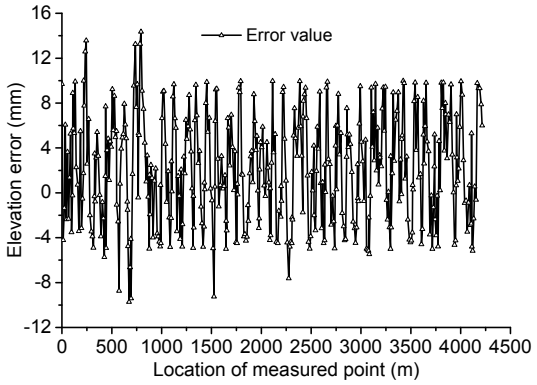

Fig. 10 Elevation errors of #1 to #7 steel box girders of the non-navigable bridge after installation

5 Conclusions

In this paper, the geometric state control indexes, that is the manufacturing parameters of top and bottom slabs, the width of annular joints of large-segment steel box girders, and the support positions, of large-segment steel box girders were determined. The geometric state equation and state transfer matrix of large-segment steel box girders under different states were deduced by taking the mileage and elevation of control points as basic state variables. The measurement data show that the difference between the width of the annular joint of the top and bottom slabs was less than 2 mm in the stress state, the eccentricity of bridge support was less than 20 mm, and the elevation error of the bridge deck was within −10 to +15 mm, which met the control accuracy requirements.

The geometric state control method, which takes the mileage and elevation of the control points of a bridge as the basic state variables, can realize the control of complex geometric relation transmission in the process of bridge construction. This method is universal and can be further applied to the geometric state control of the bridge construction of ectopic installation and multi-state conversion, such as incremental launching construction and segmental assembling construction.

Contributors

Jin-feng WANG provided the idea. Hua-wei XIANG wrote the manuscript. Jiang-tao ZHANG and Tian-mei WU helped to process the corresponding data. Rong-qiao XU helped to revise the final version.

Conflict of interest

Jin-feng WANG, Hua-wei XIANG, Jiang-tao ZHANG, Tian-mei WU, and Rong-qiao XU declare that they have no conflict of interest.

References

Arici M, Granata MF, 2007. Analysis of curved incrementally launched box concrete bridges using the Transfer Matrix Method. *Bridge Structures*, 3(3-4):165-181. https://doi.org/10.1080/15732480701510445

Breen JE, 1985. Controlling twist in precast segmental concrete bridges. *PCI Journal*, 30(4):86-111. https://doi.org/10.15554/pcij.07011985.86.111

Chen DW, Zheng XG, Xiang HF, 1993. A construction control system for P.C. cable-stayed bridges. *China Civil Engineering Journal*, 26(1):1-11 (in Chinese). https://doi.org/10.15951/j.tmgcxb.1993.01.001

Li CX, He J, Dong CW, et al., 2015. Control of self-adaptive unstressed configuration for incrementally launched girder bridges. *Journal of Bridge Engineering*, 20(10): 04014105. https://doi.org/10.1061/(ASCE)BE.1943-5592.0000709

Li Q, Bu YZ, Zhang QH, 2009. Whole-procedure adaptive construction control system based on geometry control method. *China Civil Engineering Journal*, 42(7):69-77 (in Chinese).

Lin JP, Wang JF, Chen CL, et al., 2014. Geometric shape control of trough steel girder composite bridge constructed by incremental launching method. *Bridge Construction*, 44(4):102-106 (in Chinese).

Lin YP, 1983. Application of Kalman's filtering method to cable stayed bridge construction. *China Civil Engineering Journal*, 16(3):7-14 (in Chinese). https://doi.org/10.15951/j.tmgcxb.1983.03.002

Meng FC, Liu MH, Wu WS, et al., 2014. The design philosophy and bridge's technical innovation of Hong Kong-Zhuhai-Macau Bridge. *Engineering Sciences*, 17(1): 27-35 (in Chinese). https://doi.org/10.3969/j.issn.1009-1742.2015.01.004

Muller J, 1975. Ten years of experience in precast segmental construction. *PCI Journal*, 20(1):28-61. https://doi.org/10.15554/pcij.01011975.28.61

Rosignoli M, 1997. Solution of the continuous beam in launched bridges. *Proceedings of the Institution of Civil Engineers-Structures and Buildings*, 122(4):390-398. https://doi.org/10.1680/istbu.1997.29828

Seki F, Tanaka S, 1991. Construction control system for cable-stayed bridges. *Proceedings of IABSE*, 64:286-287. http://doi.org/10.5169/seals-49315

Taylor PR, 1986. Annacis bridge superstructure–a major composite cable-stayed bridge. Annual Conference RTAC, p.89-105.

Thomson WT, 1950. Matrix solution for the vibration of non-uniform beams. *Journal of Applied Mechanics*, 17: 337-339.

Wada K, Takano H, Tomita N, et al., 1991. Construction of the Yokohama Bay Bridge superstructure. IABSE Symposium Leningrad, 64:177-182.
http://doi.org/10.5169/seals-49293

Wang JF, Lin JP, Xu RQ, 2015. Incremental launching construction control of long multispan composite bridges. *Journal of Bridge Engineering*, 20(11):04015006.
https://doi.org/10.1061/(ASCE)BE.1943-5592.0000737

Yan DH, Chen CS, Dong DF, et al., 2012. Control of self-adaptive zero-stress configuration for long-span cable-stayed bridge with steel main girders. *China Journal of Highway and Transport*, 25(1):55-58 (in Chinese).
https://doi.org/10.19721/j.cnki.1001-7372.2012.01.009

Zhong WX, Liu YF, Ji Z, 1992. Control and adjustment of cable tension in the construction of cable-stayed bridge. *China Civil Engineering Journal*, 25(3):9-15 (in Chinese).

中文概要

题　目：基于几何状态传递的大节段钢箱梁吊装施工控制

目　的：采用吊装施工的大节段钢箱梁属于整孔异位安装，其几何状态从工厂到桥址不断转换、几何关系复杂，且对成桥梁面标高、海上大节段环缝对接以及桥梁支座定位均有非常高的精度要求。本文研究基于几何状态传递的大节段钢箱梁吊装施工控制方法，以解决分阶段施工桥梁在施工过程中的几何状态控制难题。

创新点：1. 确定大节段钢箱梁几何状态控制指标，即顶底板下料参数、大节段环缝宽度和支座定位；2. 提出以钢箱梁控制点的里程和高程作为基本状态变量，推导大节段钢箱梁各状态下的几何状态方程和状态传递矩阵。

方　法：1. 针对大节段钢箱梁吊装施工特点，进行状态分析，提出其施工过程的典型几何状态，即设计成桥状态、无应力状态、工厂组拼状态和安装状态；2. 通过理论推导，构建各几何状态间的状态传递方程，得出大节段钢箱梁吊装施工时结构的几何状态变化关系；3. 基于上述推导的方程，计算大节段钢箱梁下料参数、大节段钢箱梁环缝宽度和支座定位参数，以指导施工；4. 在施工过程中对桥梁结构实际响应数据进行测试，并将实测值与理论值进行分析对比，以验证本文方法的可行性和有效性。

结　论：1. 采用本文方法实现了港珠澳大桥大节段钢箱梁有应力状态下顶底板环缝宽度差值在 2 mm 以内、桥梁支座就位后的偏心距在 20 mm 以内以及成桥梁面高程误差范围为−10 mm~+15 mm，满足控制精度要求。2. 以桥梁结构控制点的里程和高程作为基本状态变量的几何状态控制方法可实现桥梁施工过程中复杂几何关系传递的控制。3. 本文方法具有通用性，可进一步推广应用于逐孔顶推、节段拼装等异位安装以及多状态转换的桥梁施工过程的几何状态控制。

关键词：大节段钢箱梁；海上吊装；施工控制；几何状态；传递矩阵